

Discovering Pressure Modes in Ice-induced Vibrations Using Proper-Orthogonal Decomposition

Ersegun Deniz Gedikli*, Torodd Skjerve Nord*

***Sustainable Arctic Marine and Coastal Technology (SAMCoT), Centre for Research-based Innovation (CRI), Norwegian University of Science and Technology (NTNU), Trondheim, Norway, deniz.gedikli@ntnu.no, torodd.nord@ntnu.no**

Abstract

In this work, we use proper-orthogonal decomposition (POD) method to decompose an ensemble of pressure field data into spatiotemporal modes that gives insights into pressure distributions in the ice-induced vibration experiments. In the analysis, we use the Test-4300 within the Deciphering Ice-Induced Vibrations (DIIV) test campaign illustrating intermittent crushing with the ice speeds of 20 and 30 *mm/s*. Using an error threshold criterion, we show that first three empirical modes (hereinafter called pressure modes) represent most of the dynamics within the dataset. Although, this method successfully identifies the pressure modes in frequency lock-in and at low ice speeds in intermittent crushing, we only concentrate on low ice speeds in this paper for clarity.

Keywords: Ice-Induced Vibrations, POD, Pressure

1. Introduction

Ice-induced vibration (IIV) is an inherent problem seen in many offshore structures (i.e., oil platforms, offshore wind turbines) located in ice infested waters.

Offshore structures in the Arctic and Subarctic regions may interact with the ice (i.e., level ice, deformed ice etc.) which may cause ice-induced vibrations. This type of interaction is very dangerous since it may decrease the operational time significantly and may give fatigue related damages to the structures, which potentially costs significant amount of money to the offshore industry. Therefore, IIV has a growing interest not only within the research community, but also in the offshore industry.

IIVs first reported in the work of Blenkarn (1970) where full-scale observations of different structures in Cook Inlet, Alaska have been made. Later, many efforts have been made to understand such complex interactions through laboratory model tests (i.e., Kärna et al., 2003a, 2003b, Sodhi, 2001, Barker et al.,

2005, Wells et al., 2011, Määttänen et al., 2012, Nord et.al, 2015 etc.) and field tests (i.e., Määttänen, 1975, Frederking et al., 1986, Bjerkås et al., 2013 etc.).

Among those, Sodhi (2001) conducted experiments on a flexible structure, where he showed that at low indentation speeds, local pressures on the structure simultaneously increased. As the indentation speed increased, the pressure distribution on the structure also changed and at the onset of the failure, the pressure varied during failure period. These observations lead a scientific question: “Is there a global pressure distribution exist in different dynamic modes on the structure? If yes, how can we quantify such coherent distributions?” In order to answer this question, we use a well-known multivariate analysis method called proper orthogonal decomposition (POD) which is also known as principal component analysis (PCA), singular value decomposition (SVD), and Karhunen-Loeve decomposition in different research areas (see section 2.2). Our approach to the problem resembles to the approach that have generally been used in the experimental fluid mechanics community (Berkooz et al., 1993, Epps and Techet, 2010 etc.) where the method has been used to analyze particle image velocimetry (PIV) data. In the present study, we apply POD to the three-dimensional pressure dataset and reveal organized patterns within the pressure data, which we name as pressure modes. These modes are commonly referred as coherent flow structures in fluid mechanics.

2. Experiments

In the present study, one set of experimental data was analyzed in DIIV. The DIIV campaign was initiated by Norwegian University of Science and Technology (NTNU) in the beginning of 2011 to understand the complex ice-induced vibrations through model tests. Scale-model tests were conducted in the EU HYDRALAB at the Hamburg ship model basin (HSVA) ice-tank facility in Hamburg, Germany. In the experiments, ice and structural parameters were systematically investigated in a well-defined test setup as described in Määttänen et al. (2012).

2.1. Relevant Data

Of particular interest, we chose different failure modes from Test-4300 of DIIV campaign. In Test-4300, we analyzed the ice speeds of 20 and 30 mm/s , which represent two low ice speed intermittent crushing modes.

As a result, we are interested in how pressure due to the ice is distributed spatiotemporally and how pressure modes look like.

In Test-4300, the structure had a natural frequency of 12.2 Hz and diameter of 220 mm where ice drift was systematically varied between the ice velocity values of 10-320 mm/s (Nord et al., 2015). The pressure at the ice-structure interface was measured with a tactile sensor, whereas responses were measured by accelerometers, lasers and strain gauges, with a sampling frequency of 100 Hz .

2.2. POD analysis

POD is a mathematical matrix decomposition method that helps to characterize the coherent structures in a dataset. It is widely used for modal analysis, modal order reduction and characterization of both linear and non-linear systems (Berkooz et al., 1993, Feeny and Kappagantu, 1998, Gedikli et al., 2017, Kerschen et al., 2005, Ma et al., 2001). Although POD is a linear approach, it is also applied to the nonlinear problems since it does not violate the physical laws of linearization methods as shown in Berkooz et al. (1993).

Derivation of the POD method is straightforward. Let D be $m \times n$ zero mean data matrix, where m represents snapshots and n represents position state variables. In POD, we are looking for base functions $p_n(t)$ and $\chi_n(x)$, which describe the original data matrix best in least squares sense. Data matrix can be written as:

$$D(x, t) = \sum_{n=1}^{\infty} p_n(t)\chi_n(x) \quad (1)$$

where $D(x, t) \in \mathbb{R}^{m \times n}$, and $\chi_n(x)$ represents the orthonormal basis functions (modes) and $p_n(t)$ represents corresponding time coordinates. A detailed derivation of this method can be found in many studies such as Berkooz et al. (1993), Cruz et al. (2005) and many more.

Geometrically, the meaning of POD is simple. A scalar field sampled in time can be imagined as a cloud of points in a n -dimensional space, where n is the number of spatial sampling points. In this space, POD fits the best ellipsoid to this cloud of points in the least squares sense where the directions of semi-principal axes give proper orthogonal modes (POM) and the squared magnitudes of the semi-principal axes correspond to the variance of the projection points on the subspace span by the corresponding axes and represent proper orthogonal values (POV). Therefore, POD provides energy optimal reduction in dimension in the least-squares sense.

In our current dataset, we have a three-dimensional pressure data where pressure fluctuation is sketched as in Fig.1. When an ice sheet hits the structure, it creates a high-pressure zone on the structure. As this ice-structure interaction continues, this pressure may move not only up and down (structural depth), but also on the circumference of the structure. Therefore, in the analysis, pressure varies not only in the xy phase space but also in the direction of structural depth (into the paper).

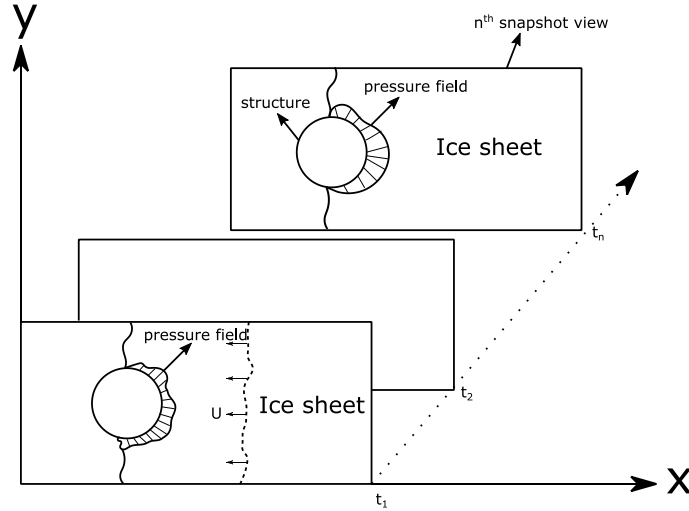


Fig. 1. Example illustration of the ice-structure interaction with varying pressure field as snapshot. Structure is fixed and ice sheet moves from right to left (in the negative x direction) with speed of U m/s.

Suppose that pressure variation has the form of $\mathbf{d} = [x, y]$. So, fluctuating pressure components of the snapshots can be written as a one data matrix as; $\mathbf{D} = [\mathbf{d}_1 \mathbf{d}_2 \dots \mathbf{d}_N]$. In other words, each snapshot of pressure fluctuations has been reorganized and arranged into two-dimensional $m \times n$ data matrix where m 's size is equal to the size of xy .

Since, in POD we solve the eigenvalue of the auto covariance matrix, we first calculate the auto covariance matrix as:

$$\mathbf{A} = \mathbf{D}^T \mathbf{D} \quad (2)$$

where T represents transpose.

Next, one can solve the eigenvalue problem of \mathbf{A} as:

$$\mathbf{A} \mathbf{V}_i = \lambda_i \mathbf{V}_i \quad (3)$$

where \mathbf{V} represents the eigenvector matrix, and λ represents the corresponding eigenvalues. Then, eigenvalues and corresponding eigenvectors are sorted in descending order. This step is very important because, it allows us to sort the modes where most dominant (coherent) structures will be in the first subspace dimensions.

Then, projecting the eigenvectors onto the data matrix and normalizing them to unit magnitude gives the corresponding proper orthogonal modes (POMs). Then, by reshaping the two-dimensional matrix back to the three-dimensional matrix, one can illustrate the coherent structures that are active in the system. Mathematically, any i^{th} POD mode of χ_i may be found calculating the following equation:

$$\chi_i = \frac{\sum_{n=1}^N V_{i,n} \mathbf{d}_n}{\|\sum_{n=1}^N V_{i,n} \mathbf{d}_n\|} \quad (4)$$

where $= 1, 2, \dots, N$, $V_{i,k}$ represents the n^{th} eigenvector corresponding to i^{th} eigenvalue. Then, one can also compute the basis function of $p_n(t)$ in Eq.1 by projecting the pressure field onto the POMs (see

Eq.5). This basis function is also known as proper orthogonal coordinates (POCs). Forming a POM matrix of $\phi = [\chi_1, \chi_2, \chi_3, \dots, \chi_N]$, one can calculate the POCs as:

$$\mathbf{p}_n = \phi^T \mathbf{d}_n \quad (5)$$

Original data can be reconstructed using any first r POMs (with rank r approximation where $r < N$):

$$\mathbf{D}_r(x, t) = \phi_r(x) \mathbf{p}_r(t) \quad (6)$$

Eigenvalues of the auto covariance matrix are generally referred as energies corresponding to the POMs in fluid mechanics since it is related to fluid's kinetic energy (see Chatterjee, 2000). Although, we do not attempt to relate the fluid characteristics to the pressure characteristics in this study, it is assumed that distributed pressure variation on a structure resemble to flow variations in a system.

The quality of the reconstruction (mode energy) can be found using the singular values (eigenvalues):

$$E_r [\%] = \frac{\lambda_r}{\sum_{n=1}^N \lambda_n} \quad (7)$$

where E represents energy and r is the rank (number of modes used in the reconstruction). Solution to this equation gives the energy fraction of each possible modes. We use the term singular value here because squares of the singular values in singular value decomposition are equal to eigenvalues of the covariance matrix (see Chatterjee, 2000). In other words, singular values presented here represent the eigenvalues of the auto covariance matrix. Alternatively, the eigenvalues can be sorted logarithmically and the energy difference between each mode can easily be seen on a logarithmic plot. In this study, we use the second method as an illustration of the modal contributions.

3. Results and Discussion

In this section, we analyze the intermittent crushing in the Test-4300 within the DIIV campaign. In the analyses, zero-mean pressure responses were obtained using Butterworth 8th order high-pass filters with 1 Hz cut-off frequency. The cut-off frequency was chosen based on the visual inspection of the frequency response so that it is sufficient to cancel the zero frequencies. Therefore, zero-mean response is attributed to the dynamic pressure variations and mean component is attributed to the static pressure on the structure. Due to the fact that ice can behave ductile and brittle depending on the relative indentation speed between ice and structure, the load build up and unloading phase are very different during intermittent crushing. During load build up, the relative speed between the indenter and ice is close to zero, the contact area and pressure grow, which cause ductile deformation of the ice. Upon ice fracture, the relative speed between ice and structure increases with orders of magnitude, and causes brittle ice failure hence a sharp load drop.

Two different time series of intermittent crushing were analyzed at 20 and 30 mm/s ice speeds, respectively. Both time series had 1500 samples from 2288 sensels, and time history of the force displayed the classical saw-tooth type of response.

3.1. Intermittent crushing at ice speed of 30 mm/s

Fig.2 illustrates the original and high-pass filtered time histories of the pressure sums on the structure. As one can clearly see, applied filter successfully moves the mean to zero-value, which is very important to analyze the dynamic variations.

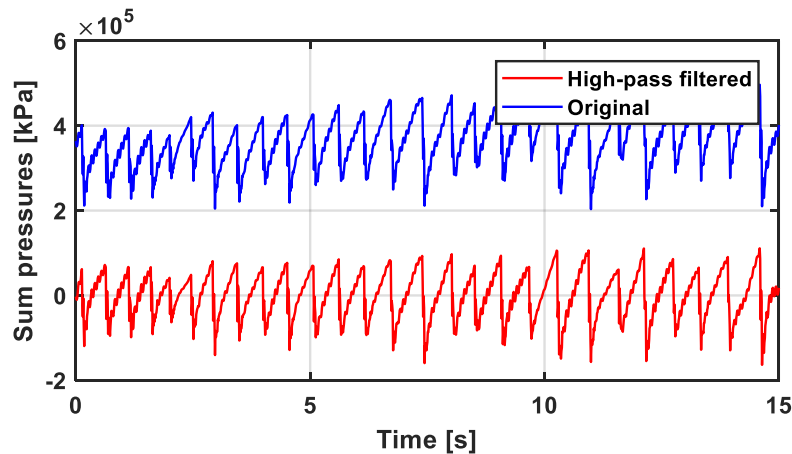


Fig. 2. Time history of the response at 30mm/s. Blue: Original response. Red: High-pass filtered response at cut-off frequency of 1Hz.

Fig.3 shows the singular values and corresponding POMs. As one can see, first singular value is significantly larger than other singular values suggesting that the first mode is the most dominant mode. Since, POD sorts the modes based on their energies in the descending order, it means that POM in the second subspace dimension is the second most dominant mode and so on. Right image in Fig.3 illustrates the corresponding POMs. As expected, pressure distribution has a line shape on the structure in the first subspace dimension. This pressure mode represents the most dominant distribution and representative of the ductile load build up on the structure. As the subspace dimension increased, the contribution of the higher order modes decreases. Second and third POM shows the dynamic variations of the pressure on the structure. Since, these modes are representative of orthogonal directions; it is believed that they represent the pressures in the orthogonal directions. In fact, when comparing the POD coefficients of the first three modes to the structural response, it was found that second and third mode contained peaks at frequencies coinciding with cross-flow vibrations of the structure. This also supports the idea that higher order modes are related to the dynamic pressure variations in the orthogonal directions.

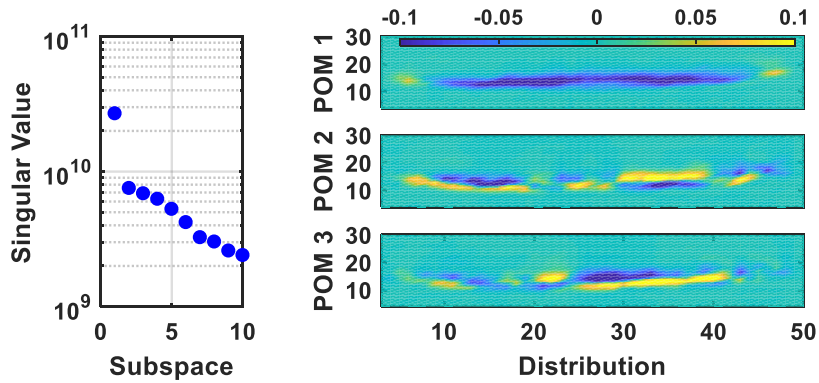


Fig. 3. Left image: Logarithmic distribution of the singular values for the first 10 subspace dimensions at the ice speed of 30mm/s . Right image: First three POMs. Colors indicate the normalized pressure variation.

Fig.4 shows the original and reconstructed signals using first three POMs. Normalized root-mean-squared-error (NRMSE) was computed for the original and reconstructed signals, and then the resulting solution was normalized with the maximum variation (height) in the original data. As a result, one can see that rank-3 approximation of the sum of the pressure at ice speed of 30mm/s results very good accuracy with the NRMSE value of 0.055 (only 5.5% of reconstruction error). This result supports the argument presented for Fig.3 where first three POMs represent the total dynamic and static pressure variations on the structure with close to 94% accuracy.

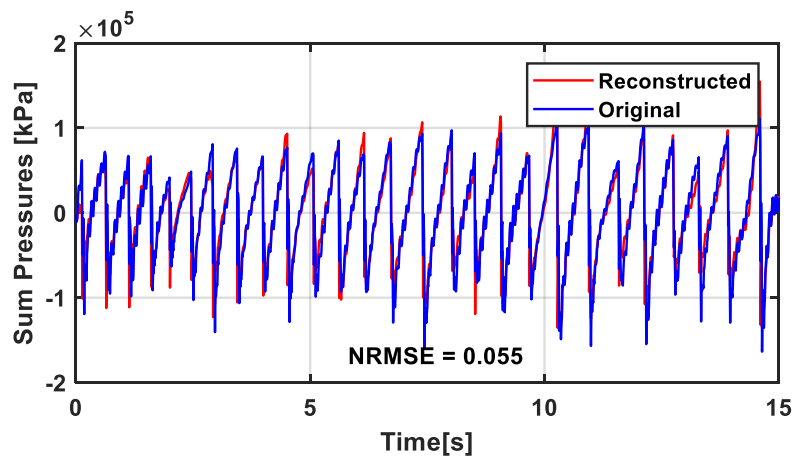


Fig. 4. Original time history of the pressure with the reconstructed pressure using first three POMs at ice speed of 30mm/s .

3.2. Intermittent crushing at ice speed of 20mm/s

Fig.5 illustrates the original and high-pass filtered time histories of the pressure sums on the structure at the ice speed of 20mm/s . Similar to previous case, used filter successfully moves mean to zero.

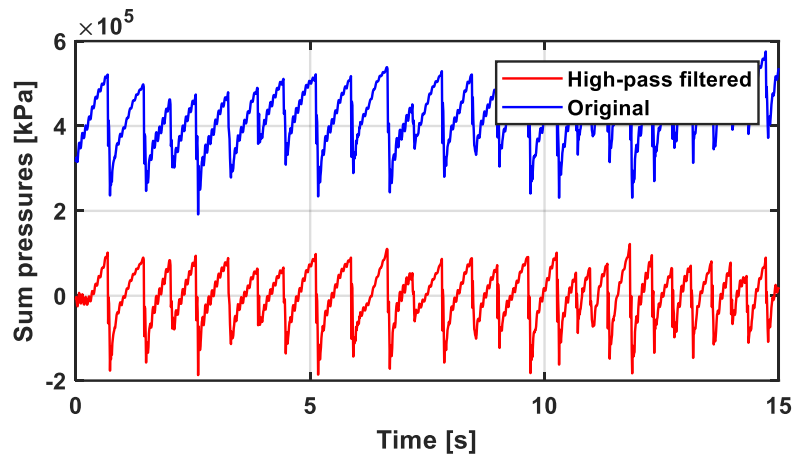


Fig. 5. Time history of the response at 20mm/s. Blue: Original response. Red: High-pass filtered response at cut-off frequency of 1Hz.

Fig.6 illustrates the computed singular values in descending order and corresponding first three POMs. From the left image in Fig.6, one can clearly see that first singular value is significantly larger than second singular value. Although, second and third singular values are very close to each other, there is a jump between the third and higher order modes. Since singular values were sorted in descending order, one can say that energy in the first POM is larger than second POM, and energy in the second mode is larger than third POM and so on. Right image in the Fig.6 shows that first POM resembles to a line shaped pressure mode where pressure was distributed along the circumference of the structure. Second POM in this case resemble to the second POM at 30 mm/s where pressure varies in two directions (similar to traveling wave type of response). However, third POM is completely different from third POM at 30 mm/s. At lower ice speed of 30 mm/s, pressure distribution resembled to traveling type of response, which is similar to second POM at the same ice speed. However, at ice speed of 20 mm/s, third POM shows that there are two distinct line of pressures across the span. This suggests that, pressure is active in two directions at the same time at the third subspace dimension. This makes sense because, when ice hits the structure, the pressure on the structure may vary both up and down (vertically), and along the circumference of the structure (spatially) at the same time.

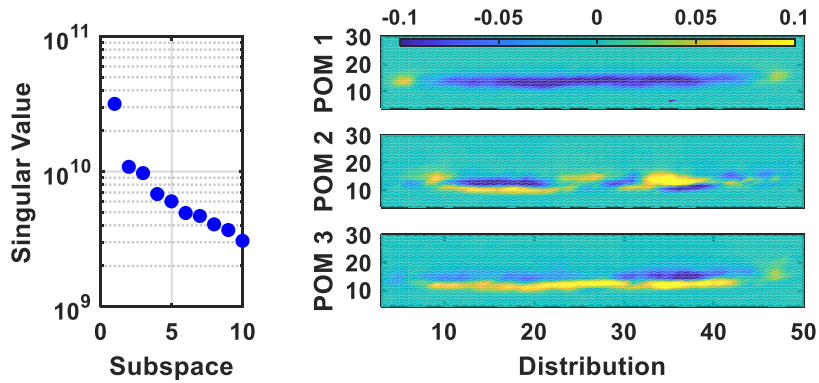


Fig. 6 Left image: Logarithmic distribution of the singular values for the first 10 subspace dimensions at the ice speed of 20mm/s . Right image: First three POMs. Colors indicate the normalized pressure variation.

Fig.7 shows the original and reconstructed signals using first three POMs. NRMSE was computed for the original and reconstructed signals, and then, the resulting solution was normalized with the maximum variation (height) in the original data. As a result, one can see that rank-3 approximation of the sum of the pressure at ice speed of 20mm/s results very good accuracy with the NRMSE value of 0.051 (only 5.1% of reconstruction error). This result supports the argument presented for Fig.3 and Fig.6 where first three POMs represent the total dynamic pressure variations on the structure.

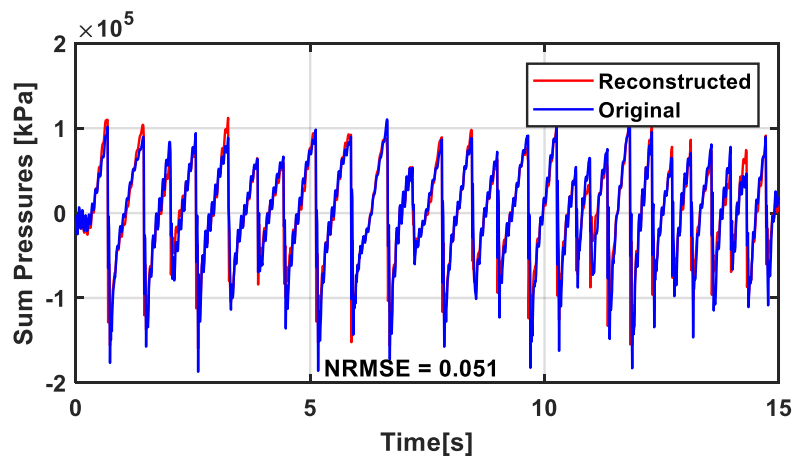


Fig. 7. Original time history of the pressure with the reconstructed pressure using first three POMs at ice speed of 20mm/s .

4. Conclusion

In this study, POD was applied to examine the pressure activity on the structure due to ice-induced vibrations. The derivation of the POD method was outlined and relationship between POC, and POM was noted. A criterion for determining the active pressures in the structure was proposed using signal reconstruction error. It was found that first POM illustrated the ductile pressure variation on the structure

therefore it is the most dominant mode and inherently it is in the direction of ice flow. First three modes confirmed that three active modes were detected in the system and one can reconstruct the original signal with less than 6% error in both cases. It is believed that higher order modes were contaminated with the added noise due to complex ice-structure interaction.

The intention of this work is not to favor one method over another. Here, we only attempt to find the pressure modes that are active in our current system. In fact, other methods such as smooth-orthogonal decomposition (Gedikli et al., 2017, Chelidze and Zhou, 2006), or dynamic mode decomposition (Tu, 2013), found to work better in a highly nonlinear system. However, these methods are relatively new and it is not clear if they work with any kind of dataset, whereas POD is an established method with many field of applications.

We also applied POD and SOD to different vibration modes in complex ice-structure interactions and analyzed the results. These results are not presented here, and they will be published in a separate journal paper.

Acknowledgement

The work described in this paper was supported by the European Community's 7th Framework Program through the grant to the budget of the Integrated Infrastructure Initiative HYDRALAB-IV, Contract no. 261520. The authors would like to thank the Hamburg Ship Model Basin (HSVA), especially the ice tank crew, for the hospitality, technical and scientific support and the professional execution of the test program in the Research Infrastructure ARCTECLAB.

References

- Barker, A., Timco, G., Gravesen, H., Vølund, P.** (2005), Ice loading on Danish wind turbines: part 1: dynamic model test. *Cold Reg. Sci. Technol.* 41 (1), 1-23.
- Berkooz, G., Holmes, P., and Lumley, J.L.** (1993), The Proper Orthogonal Decomposition in the Analysis of Turbulent Flows, *Annual Review of Fluid Mechanics*, Vol. 25(1), pp. 539-575
- Bjerkås, M., Meese, A., Alsos, H.S.** (2013), Ice induced vibrations- observations of a full-scale lock-in event. *Proceedings of the Twenty-Third International Offshore and Polar Engineering*, International Society of Offshore and Polar Engineers (ISOPE), Anchorage, Alaska, pp. 1272-1279.
- Blenkarn, K.A.** (1970), Measurement and analysis of ice forces on Cook Inlet structure, *Offshore Technology Conference*, Houston, TX, pp.365-378.
- Chatterjee, A.** (2000), An introduction to the proper orthogonal decomposition, *Special section in Computational Science*, Vol. 78, No. 7
- Chelidze, D., Zhou, W.** (2006), Smooth Orthogonal Decomposition-Based Vibration Mode Identification, *Journal of Sound and Vibration* 292, no. 3, pp: 461-473.
- Cruz, A.S., David, L., Pecheux, J., and Texier, A.** (2005), Characterization by proper-orthogonal-decomposition of the passive controlled wake flow downstream of a half cylinder, *Exp. Fluids* 39, 730.

INT-NAM 2018 3rd International Symposium on Naval Architecture and Maritime
Yildiz Technical University, Istanbul, Turkey

- Feeny, B.F. and Kappagantu, R.** (1998). On The Physical Interpretation of Proper Orthogonal Modes In Vibrations, *Journal of Sound and Vibration*, 211(4), pp. 607-616.
- Frederking, R., Haynes, F.D., Hodgson, T.P., and Sayed, M.** (1986), Static and dynamic ice loads on the Yamachiche lightpier, 1984-1986, 8th International Symposium on Ice, IAHR Iowa, USA, pp. 115-126.
- Gedikli, E.D., Dahl, J.M., Chelidze, D.** (2017), Multivariate analysis of vortex-induced vibrations in a tensioned cylinder reveal nonlinear modal interactions, *Procedia Engineering* 199, no. Supplement C, pp. 546-551
- Gedikli, E.D., Chelidze, D., Dahl, J.M.** (2018), Bending dominated flexible cylinder experiments reveal insights into modal interactions for flexible body vortex-induced vibrations. The Twenty-Eight International Offshore and Polar Engineering Conference (ISOPE), Accepted, Sapporo, Japan.
- Kärnä, T., Kolari, K., Jochmann, P., Evers, K.-U., Bi, X., Määttänen, M., Martonen, P.** (2003a), Tests on dynamic ice-structure interaction. 22nd International conference on Offshore Mechanics and Arctic Engineering (OMAE), Cancun, Mexico (paper no. 37397).
- Kärnä, T., Kolari, K., Jochmann, P., Evers, K.-U., Bi, X., Määttänen, M., Martonen, P.** (2003b), Ice action on compliant structures. VTT Research Notes 2223. VTT.
- Kerschen, G., Golinval, J.C., Vakakis, A.F., and Bergman, L.A.** (2005). The Method of Proper Orthogonal Decomposition for Dynamical Characterization and Order Reduction of Mechanical Systems: An Overview, *Nonlinear Dynamics*, Vol. 41 (1-3), pp. 147-169.
- Ma, X., Vakakis, A.F., and Bergman, L.A.** (2001). Karhunen-Loeve Modes of a Truss: Transient Response Reconstruction and Experimental Verification, *AIAA Journal*, Vol. 39, No.4, pp. 687-696.
- Määttänen, M.** (1975), Experiences of ice forces against a steel lighthouse mounted on the seabed, and proposed constructional refinements. *Port and Ocean Engineering Under Arctic Conditions (POAC)*, Fairbanks, Alaska, pp. 857-867.
- Määttänen, M., Løset, S., Metrikine, A., Evers, K.-U., Hendrikse, H., Løney, C., Metrikin, I., Nord, T.S., Sukhorukov, S.** (2012), Novel ice induced vibration testing in a large-scale facility. "Ice Research for a Sustainable Environment" (IAHR), Dalian, China (paper no. 092).
- Nord, T.S., Lorens, E.-M., Määttänen, M., Øiseth, O., Høyland, K.V.** (2015), Laboratory experiments to study ice-induced vibrations of scaled model structures during their interaction with level ice at different ice velocities.
- Sodhi, D.S.** (2001), Crushing failure during ice-structure interaction. *Eng. Fract. Mech.* 68 (17-18), 1889-1921.
- Tu, J.H.** (2013), Dynamic mode decomposition: Theory and applications. PhD Thesis: Princeton University.
- Wells, J., Jordaan, I., Derradji-Aouat, A., Taylor, R.** (2011), Small-scale laboratory experiments on the indentation failure of polycrystalline ice in compression: main results and pressure distribution. *Cold Reg. Sci. Technol.* 65 (3), 314-325.